Separation of Negatively Charged TiO_2-coated Polystyrene Beads in Microfluidic Device

Chalinee Phiphatanaphiphop,[1] Komgrit Leksakul,[1*]
Rungrueang Phatthanakun,[2] Wutthikrai Busayaporn,[2] Chatree Saiyasombat,[2] Pat Phothongkam,[2] Isa Anshori,[3] MdMohosin Rana,[3] Hiroaki Suzuki,[3]

[1]Graduate Program in Industrial Engineering, Department of Industrial Engineering, Faculty of Engineering, Chiang Mai University, Thailand 50200
[2]Synchrotron Light Research Institute (Public Organization), 111 University Avenue Nakhon Ratchasima, Thailand 30000
[3]Graduate School of Pure and Applied Sciences, University of Tsukuba, 1-1-1 Tennodai, Tsukuba, Ibaraki, 305-8573, Japan

Corresponding author *: E-mail address: komgrit@eng.cmu.ac.th

Abstract

This research was presented the special designed microfluidic device generated for sperm separation based on assumption of different surface electrical charged of sperms X and Y. However, to avoid ethical problem, the microfluidic chip has been tested with the mimic electrical charged particles, TiO_2-coated Polystyrene beads, (TiO_2-coated Ps-beads), instead of spermatozoa. The work has been separated into three main parts. Firstly, the simply but efficient fabrication of negatively charged TiO_2-coated Ps-beads has been presented. In addition, various characterization techniques such as X-ray diffraction (XRD), Tungsten Scanning Electron Microscopy (W-SEM) with energy-dispersive X-ray spectroscopy (EDS) mode, and X-ray Absorption Spectroscopy (XAS), have been reported in this work to elucidate the reasons behind the persistence of negatively charged on the surface of TiO_2-coated Ps-beads. Results show that the fabricated TiO_2-coated Ps-beads was partly coated in the mixed forms of amorphous Ti^{4+} and had caused a negatively charge to appear on the surface after fabrication and had sustained its electrical charged for long. Secondly, process of simulation and fabrication of microfluidic device was presented. Finally the negatively charged TiO_2-coated Ps-beads were tested in this microfluidic devices. For design of microfluidic devices integrated with a couple of microelectrodes, the simulated structures were fabricated by photolithographic technique and tested with the Ps-beads. Percentage of validation for Ps-beads separation indicated that the 100 μm-distance-between-electrodes microfluidic device exhibits to be the highest performance prototype at 86.96%. For further confirmation, another model so called the single path prototype has been established. It is confirmed by 92.59% of validation for the utilization of the device. The successfully designed microfluidic devices can be examined with actual spermatozoa later. Furthermore, process to fabricate the negatively

charged TiO_2-coated Ps-beads can be established as testified samples for development of other microfluidic devices.

Keywords: microfluidic, microelectrodes, negatively charged, TiO_2, assisted reproductive technology

1. Introduction

Assisted Reproductive Technology (ART) gains more importance at the present time as it assists people who have infertility issues to be successful in their attempts to have biological children. In most of the cases, the infertility concerns the problem of inability of sperms to fertilize an oocyte naturally [1]. Intracytoplasmic sperm injection (ICSI) and traditional *in vitro* fertilization (IVF) were introduced as solutions to this problem. However, ICSI and IVF are not applicable in cases of low sperm count, low sperm motility, or cryopreserved samples of sperm with reduced motility [2-4]. Furthermore, the success of these techniques is highly subjective and dependent on the skill of the embryologist. To improve the rate of success, microfluidic systems have been proposed as bio-sensing devices for sorting, manipulation, detection, and characterization of sperms [5-9]. With regard to sorting of sperms for sexual selection in fertilization, [10] reported evidence of slight difference in the electrical charge caused the variation of electrophoretic mobility between sperms those carrying chromosome X and Y. Therefore, fabrication of microfluidic devices that are capable of sorting sperms for sexual selection becomes a significant topic [11]. In this work, fabrication of microfluidic devices installed with microelectrodes in order to make them capable of separating sperms is reported. However, to avoid ethical problems and difficulties to utilize the devices with real sperms in the development stage, device examination has been conducted with negatively charged TiO_2-coated Polystyrene beads (TiO_2-coated Ps-beads). Methods to create negatively charged TiO_2-coated Ps-beads also are presented . After that, the Ps-beads were characterized by various characterization techniques. Then, simulation and fabrication of the microfluidic devices have been shown. Finally, the microfluidic devices with microelectrodes were examined to separate the negatively charged TiO_2-coated Ps-beads to evaluate percentage of validities.

2. Materials and methods

2.1. *Fabricated TiO_2-coated Ps-beads*

Polystyrene beads (Ps-beads) cat No. PP-50-10 at size 5.98 μm obtained from Spherotech Inc. were transferred into an Eppendorf tube containing ethanol solution in the ratio of 100:1000 μl. A micropipette was used to collect 10 μl of beads then spread on the glass. The beads were left to dry for 30 min. Then, Ti was sputtered on the beads for around 15 min. After that, O_2 plasma was employed at 100 W of RF power with 30 Pa of pressure for 3 min. The beads were removed from the glass substrate with 12 ml of EtOH by sonication for 5 sec each time and transferred to the solution in the Eppendorf tube (1 ml of solution in each

Eppendorf tube). Then, the tube was centrifuged for 15 sec and the supernatant was removed. Finally, DI 1 ml of DI water was added to make the stock of TiO_2-coated Ps-beads.

2.2. *Characterization of TiO_2-coated Ps-beads*

2.2.1. *XRD and SEM-EDS*

Crystalline structure and phase identification of TiO_2-coated Ps-beads were examined by XRD experiment using a Rigaku SmartLab 9KW with Cu K_α radiation (λ = 1.5406 Å) to generate X-rays with a voltage of 40 kV and a current of 30 mA. Parallel beam mode was employed with incident slit at 1 mm width, length limit slit at 10 mm, and receiver slit at 20 mm. The XRD patterns were collected from 5° to 80° with increments of 0.02° and a scan rate of 3.0°/min. Tungsten scanning electron microscopy (W-SEM) was performed by FEI at 20 kV acceleration voltage. The W-SEM images were captured under secondary electron mode in a high vacuum environment. Note that the pictures of the surfaces have been captured without any deposited element on the sample, which presents the electrical conductivity of the surface. Furthermore, energy-dispersive X-ray spectroscopy (EDS) mode was employed for elemental investigation of specific areas of the surface.

2.2.2. *XAS*

The oxidation state and local structure of TiO_2-coated PS-beads were determined by X-ray absorption spectroscopy (XAS) at beamline BL1.1w, equipped with an Si (111) double-crystal monochromator, of the Synchrotron Light Research Institute (SLRI), Thailand. The SLRI storage ring was operated at an electron energy of 1.2 GeV with the electron beam current in the range of 140–80 mA. The spectra near the Ti K-edges were measured in the transmission mode at room temperature using Ti foil, Ti_2O3, rutile-TiO_2, and anatases-TiO2 as references.

2.3. *Microfluidic device fabrication*

2.3.1. *Design and simulation*

The design of the structure for separation the negatively charged Ps-beads mimic the character of Y-shape structure. The Comsol® program was applied for simulation of the electrical field and flow of microfluidic by using mode electrostatics (es), Transport of Diluted Species (tds) and laminar flow, respectively. The simulations were calculated according to the Reynolds number equation as following;

$$\mathrm{Re} = \frac{\rho U L}{\mu}, \qquad (1)$$

where ρ is the fluid density, U is a characteristic velocity of the flow, L is a characteristic dimension of the device (mm) and μ is the fluid viscosity (1 mPa s).

While, electric displacement field nodes is established by the following electric-displacement boundary condition;

$$n \cdot D = n \cdot D_0 , \quad (2)$$

where Eq. (2) specified the normal component of the electric displacement field at a boundary and D_0 is the boundary electric displacement field (C/m^2).

In addition, calculation of fluidic transportation depends on convection and diffusion. The transportation of diluted species which considered as ionic species at interface is calculated based on migration in electric fields. Finally, the mass balance has been taken into the calculation as follows:

$$\nabla \cdot \left(-D_i \nabla c_i - z_i u_{m,i} F c_i \nabla V \right) + \mu \cdot \nabla c_i = 0 , \quad (3)$$

where c_i denotes the concentration of species i (mol/m^3), D_i is the diffusion coefficient of species i (m^2/s), u is the fluid velocity (m/s), F refers to Faraday's constant (s·A/mol), V denotes the electric potential (V), z_i is the charge number of the ionic species (unitless), and $u_{m,i}$ is ionic mobility (s·mol/kg).

The structure of microfluidic devices were designed by the Layout editor® program with various different distances between the electrodes; 30 μm, 50 μm, 100 μm, and 200 μm then named with type A to D, respectively. The parameters setting were presented as in Table 1. Then all structure (type A to D) were exported into Comsol® program and were analyzed by the Eq. (1) - (3). Finally, the electrical displacement field (c/m^2) were calculated by the program.

Table 1. Parameters setting in each types to designed the microfluidic devices used in Layout editor® and Comsol®.

Type	Electrode (mm)		Microchannel (mm)		Voltage (V)	Distance between electrodes (μm)
	Width	Height	Width	Height		
A	0.5	5	0.1	6	1	30
B	0.5	5	0.1	6	1	50
C	0.5	5	0.15	6	1	100
D	0.5	5	0.25	6	1	200

2.3.2. *Photolithography process*

The microfluidic devices integrated with the microelectrodes were fabricated by UV and soft lithography process, as illustrated in Figure 1. Cr/Pt layers were deposited on substrate by sputtering and UV patterning to make electrode patterns followed by lift-off technique to achieve the final form of electrodes, as shown in Figure 1 (a). The spin-coated of positive photoresist (S-1818G) at 500 rpm for 5 sec and 2000 rpm for 10 sec were employed. Then, the samples were baked in an oven for 30 min at 80°C and cooled down to room temperature for 15 min. UV mask to pattern the electrodes has been aligned and was irradiated with UV for 40 sec using mask aligner exposure. Next, the pattern was lifted off using toluene, which was warmed up to 30°C in water bath, to soak the substrate for 30 sec. After that, the substrate was developed by using microposit^{TM} MF-319 developer for 1 min. The sputtered Cr and Pt film was deposited on the substrate and lifted off by immersing in acetone for 1 hr. To create the microchannel, UV exposure was performed on the SU-8 25, negative photoresist and was developed to achieve the master mold for PDMS replication. The SU-8 25 was spin-coated on lime glass substrate to obtain film at thickness of 40 µm using the following conditions; 500 rpm for 5 sec, then gradually increase the speed for 10 sec to reach 1,250 rpm then remain at this speed for 10 sec. The pattern of microchannel was aligned and exposed by UV for 180 sec. After that, it was developed by SU-8 developer two times for 10 min and 20 min, respectively. Then Isopropyl alcohol (IPA) has been used for the final wash for 1 min. Therefore, the SU-8 25 has been fabricated as the mold. Next, the PDMS replicate was mixed by using PDMS precursor (KE-1300T) for 15 g and PDMS curing agent (CAT1300) for 1.5 g in a plastic cup. Then the mixed PDMS has been put in vacuum chamber to remove air bubbles in the PDMS solution. The patterned SU-8 25 mold has been placed in the frame then the PDMS mixture has been poured atop of the mold then put into the vacuum chamber 2-3 times to remove air bubbles. Next, it was baked at 80°C for 30 min then left at room temperature for 24 hours. The microchannel-pattern PDMS substrate has been peeled off the SU-8 mold and placed it on the Cr/Pt electrodes to be microfluidic chip.Finally, the microfluidic chip was connected to potentiostat and power supply to be able to apply electricity. This special designed microfluidic chip can separate the negatively charged TiO_2-coated Ps-beads those flowing pass these two electrodes.

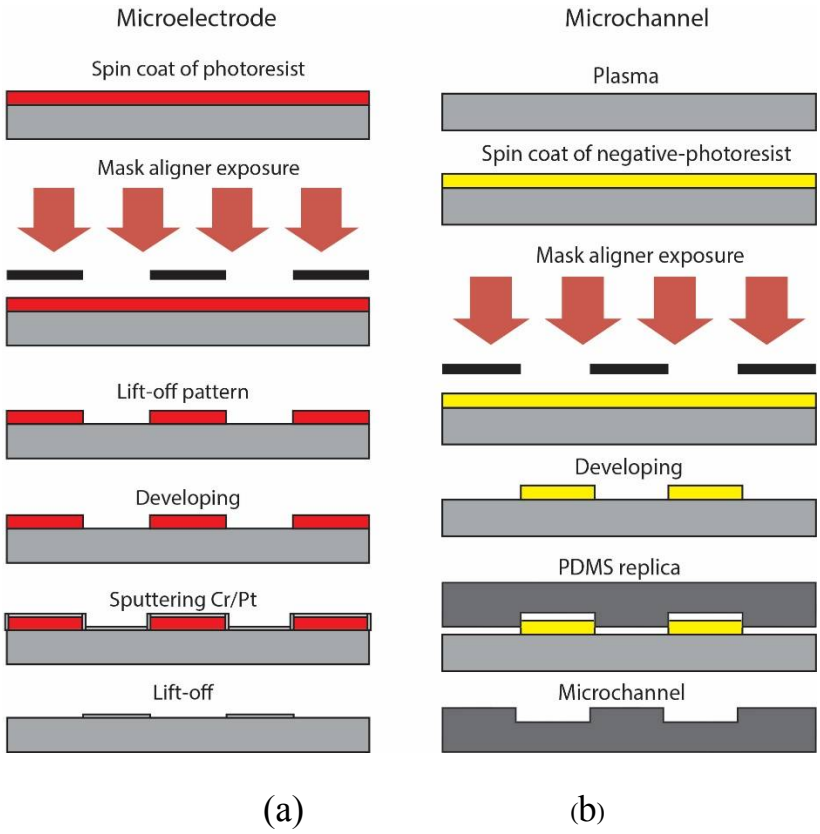

Figure 1. An illustration of the fabrication process of UV and soft lithography. (a) The microelectrodes' fabrication procedure and (b) the microchannels' fabrication procedure.

3. Result and Discussion

3.1. *TiO_2-coated Ps-beads*

3.1.1. *XRD and SEM-EDS*

As for the XRD experiment, none of the crystalline peaks of TiO_2 which were detected clearly expressed the amorphous form of the TiO_2 structure. Therefore, the result will not be shown here. The morphology of the TiO_2-coated Ps-beads was investigated; Figure 2 (a) and Figure 2 (b) show the SEM images of the TiO_2-coated Ps-beads. In Figure 2 (a), the Ps-beads appear mostly of the same size, around 5 μm in diameter. Note that at some ratios, the Ps-beads show the size to be slightly larger. Most of the Ps-beads exhibit incomplete surface coating as they are partly shelled. Figure 2 (b) shows the area as labeled in white rectangular shape in Figure 2 (a) at higher magnitudes and clearly emphasizes the partly coated surface of the Ps-beads. Moreover, elemental analysis was employed for investigation using SEM-EDS in the red rectangle areas seen in Figure 2 (b). The results reveal the

spectra of Ti and O in the area labeled as a solid red rectangle. In the dotted red rectangle area, there is no sign of Ti.

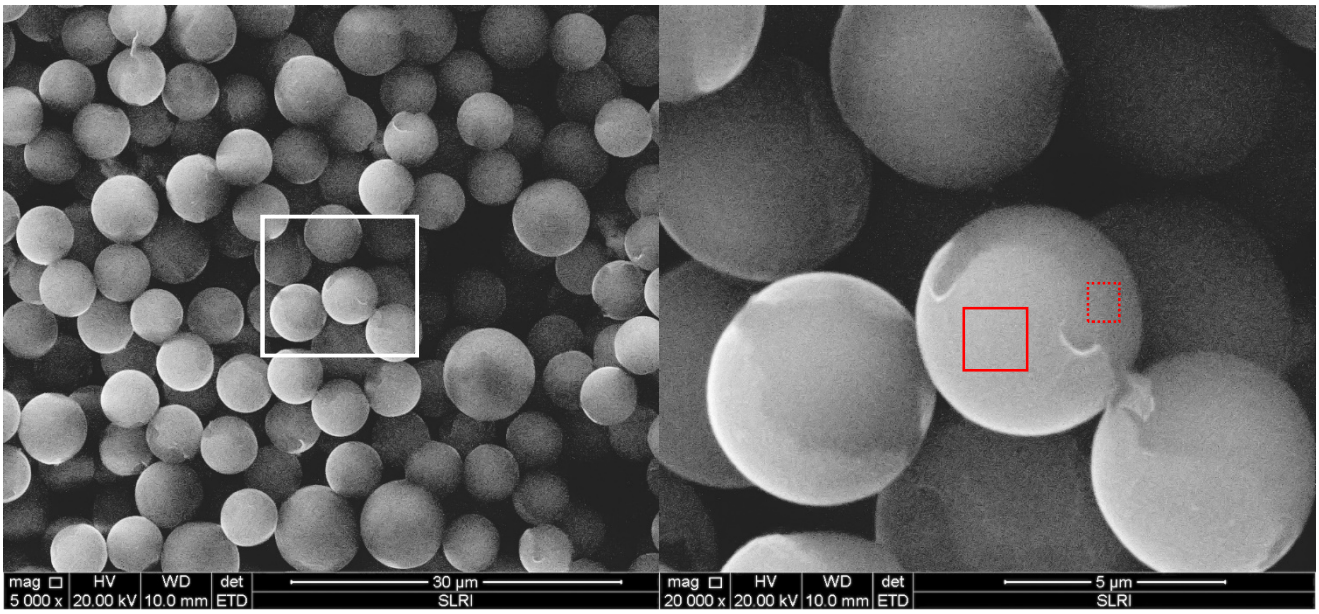

Figure 2. (a) The SEM image of TiO_2-coated Ps-beads at 5000× of magnitude. (b) 20000× magnitude of area labeled by the white rectangle in (a). SEM-EDS was used for elemental analysis for investigation of areas labeled using solid red and dotted red rectangles.

3.1.2. *XAS*

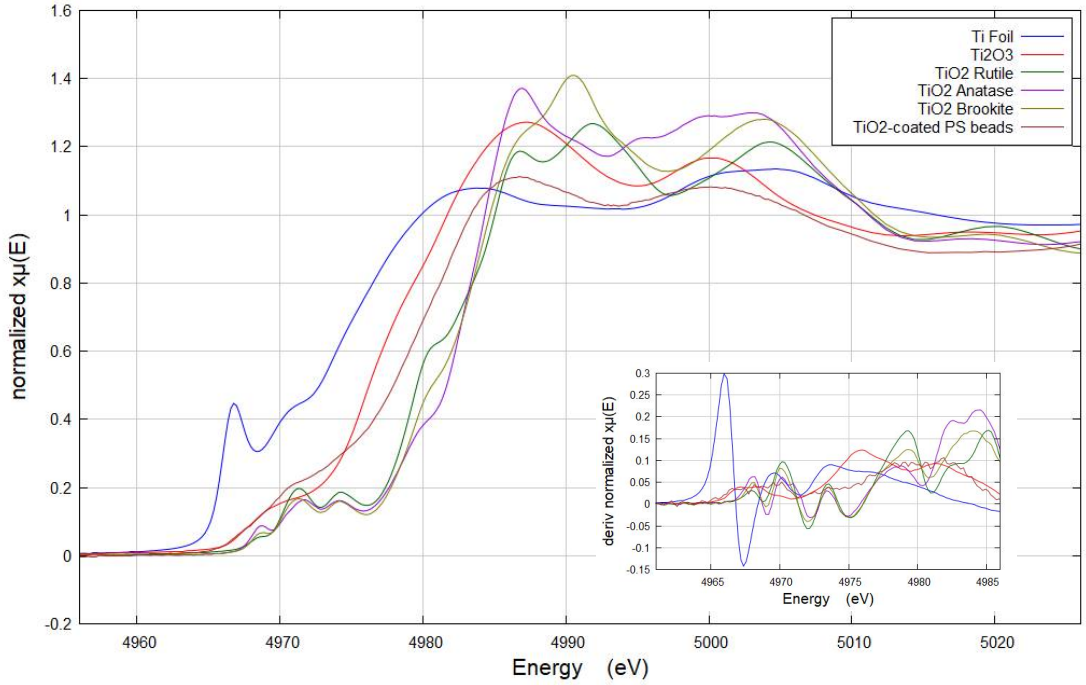

Figure 4. The Ti K-edge XANES experimental spectra of TiO_2-coated PS-beads in comparison to the references.

The XAS spectra of TiO_2-coated Ps-beads has absorption edge at 4979 eV which matches with the absorption edge of anatase-TiO_2 and rutile-TiO_2. Therefore, the oxidation number of the TiO_2-coated Ps beads clearly is Ti^{4+}. The pre-edge feature at around 4970 eV is bound-state transition, such as the 1s → 3d transition [12]. The pre-edge of TiO_2-coated Ps-beads is located at 4971 eV with 0.21 normalized pre-edge height. The position and height of the pre-edge feature directly correspond to the six-fold coordinated Ti [12-13].

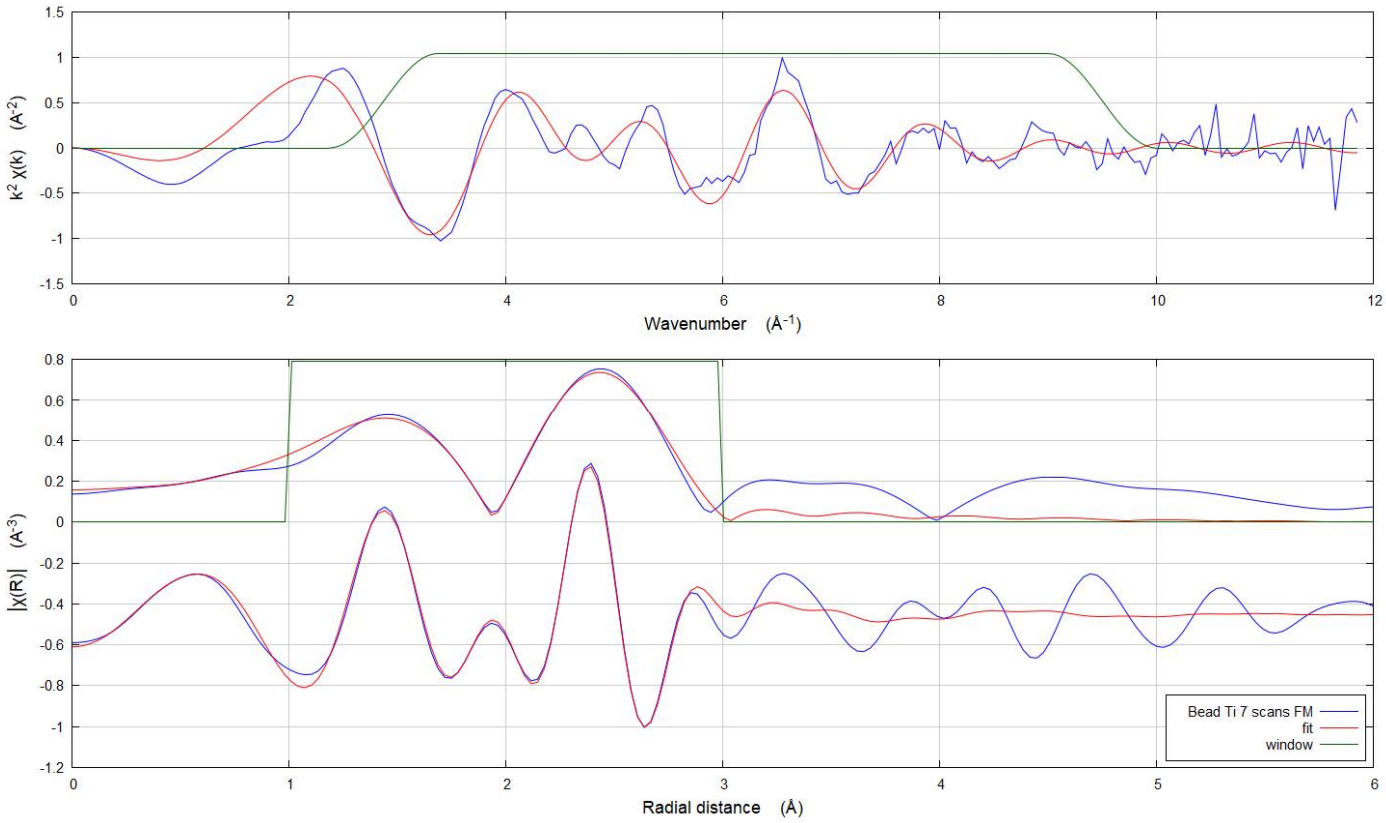

Figure 5. The $k^2\chi(k)$ functions (a) and the corresponding amplitude and real part of Fourier transforms (FT) (b) of TiO_2-coated Ps-beads. The red lines represent the simulations using the parameters shown in Table 2.

To find the distance from the nearest neighbor shell and the coordination number, the spectrumin energy space was transformed to *k* space and then transformed to *R* space using Fourier transform, as shown in Figure 5. In the R space without phase correction, the peaks at 1.5 Å and 2.4 Å were associated with O and Ti, respectively. EXAFS best-fit values were as reported in Table 2. The scattering amplitude($^{2}_{0}$) was fixed at 0.87 which was determined from anatase-TiO_2. The nearest neighbor of Ti at 2.05 ± 0.02 Å was O with highly disordered Ti–O distance and had the coordination number of 5.7 ± 2.4. This coordination number

indicated that the Ti could be in the tetrahedral site and the octahedral site. However, it is more likely that Ti was in the six-fold, coordinated as evaluated from XANES. The result leads to the conclusion that the TiO_2 coated on the surface was in the amorphous form and that it is mostly in the Ti^{4+} state with high surface area. This might be the factor that caused the negative charge to be able to appear on the surface for a long term.

Table 2. Ti K-edge EXAFS Fitted Parameters of TiO_2-coated PS-beads

Path	N_{degen}	R (Å)	σ^2 (10^{-3} Å^2)	E0 (eV)
Ti–O	5.7 ± 2.4	2.05 ± 0.02	24 ± 10	-0.04 ± 2.00
Ti–Ti	1.0[a]	2.54 ± 0.03	9 ± 1	-0.04 ± 2.00
Ti–Ti	3.0[a]	3.02 ± 0.02	9 ± 1	-0.04 ± 2.00

[a]Values without uncertainties were not determined in the fit but were held at the given value.

3.2. *Microfluidic devices*

3.2.1. Comsol® simulation

Simulation with the Comsol® program for finding out the optimal model of microfluidic devices was conducted. The result in term of electric displacement field from simulation at each distances between the electrodes at 30 µm, 50 µm, 100 µm, and 200 µm were 2.88 × 10^{-7}, 2.33 × 10^{-7}, 3.32 × 10^{-7}, and 1.02 × 10^{-7} C/m^2, respectively, as can be seen in Figure 6.

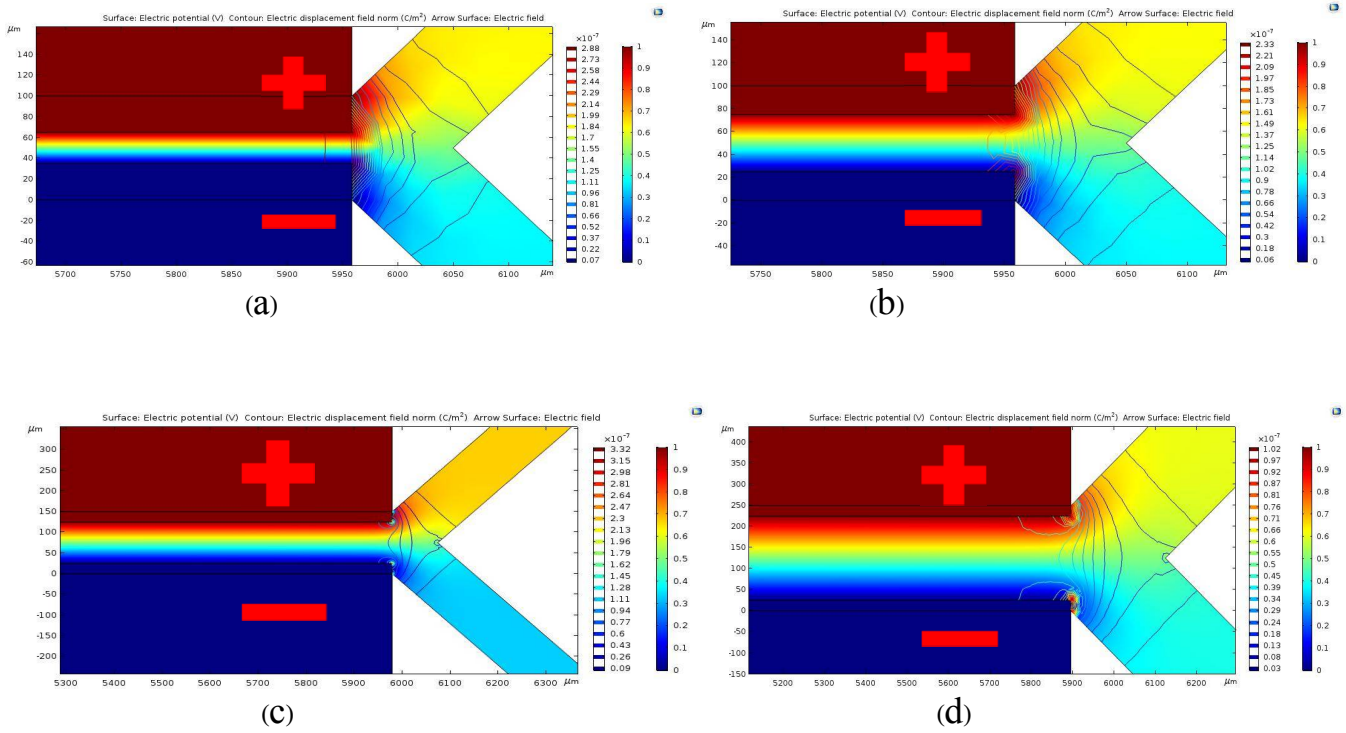

Figure 6. The result of the simulation by the Comsol® program exhibit the variation of electric displacement field at different distances between the microelectrodes.

3.2.2. Device examination: separation of TiO2-coated Ps-beads

The microfluidic chip was fabricated by photolithography process and composed of microelectrodes and microchannel as presented in Figure 7. The experiments were divided into four sets based on the different distances between the microelectrodes. The set-up of each experiments were made under microscope and the video files were recorded to investigate the performance of microfluidic devices. The video file has been presented as the supporting information (S-1). When the microfluidic devices were connected to the potentiostat to apply the potential at 1 V for 1 min, the negatively charged TiO_2-coated Ps-beads were attracted by the positive electric field in the area between the two electrodes. After that the Ps-beads were diverged to the following microchannel, as demonstrated in Figure. 8. Noted that the flow rate of fluid is at 0.1μL/sec. The examinations were repeated for 10 times. The result showed that the microfluidic device with the 100μm distance between the microelectrodes exhibits the highest performance at 86.96% validation for the separation of negatively charged TiO_2-coated Ps-beads as shown in Table 3.

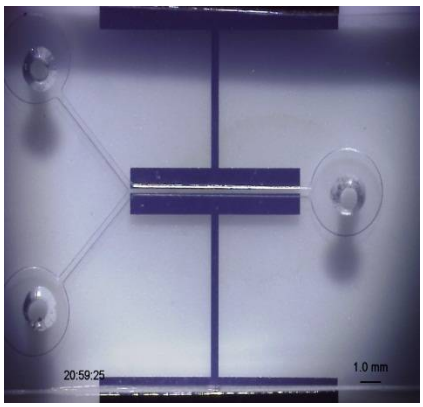

Figure 7. The completed microfluidic chip for separating negatively charged TiO_2-coated Ps-beads.

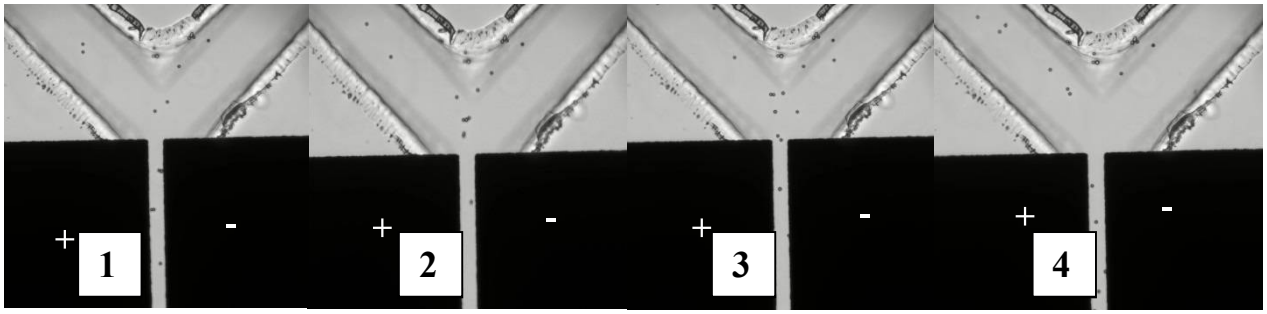

(a)

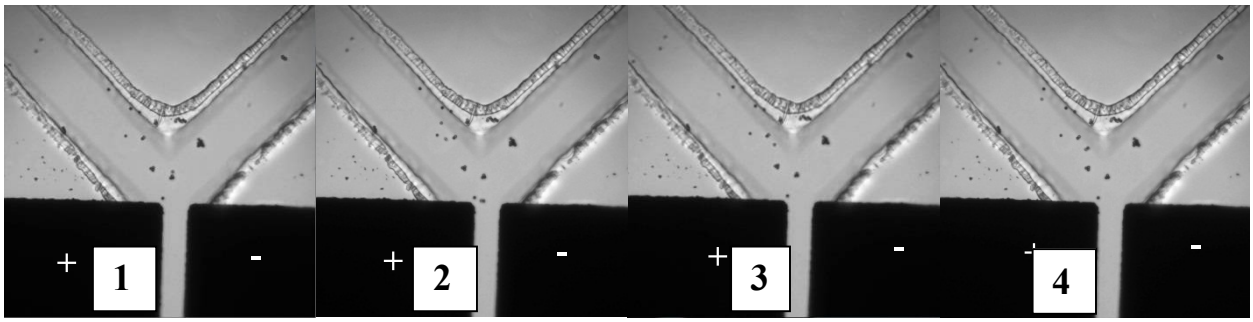

(b)

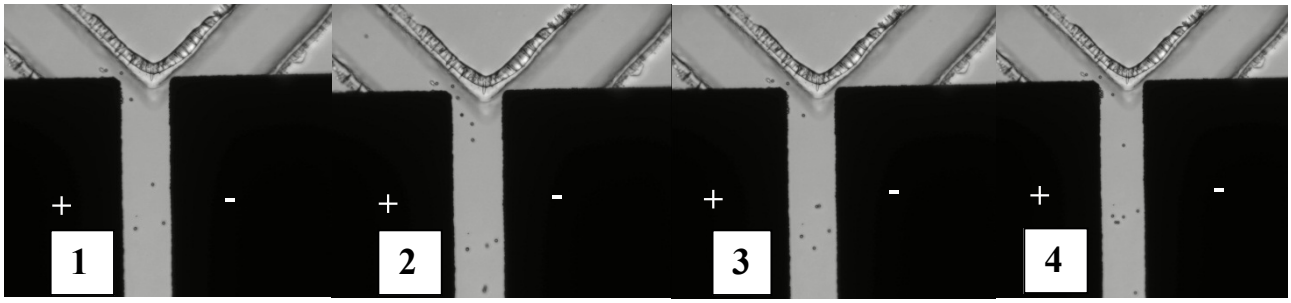

(c)

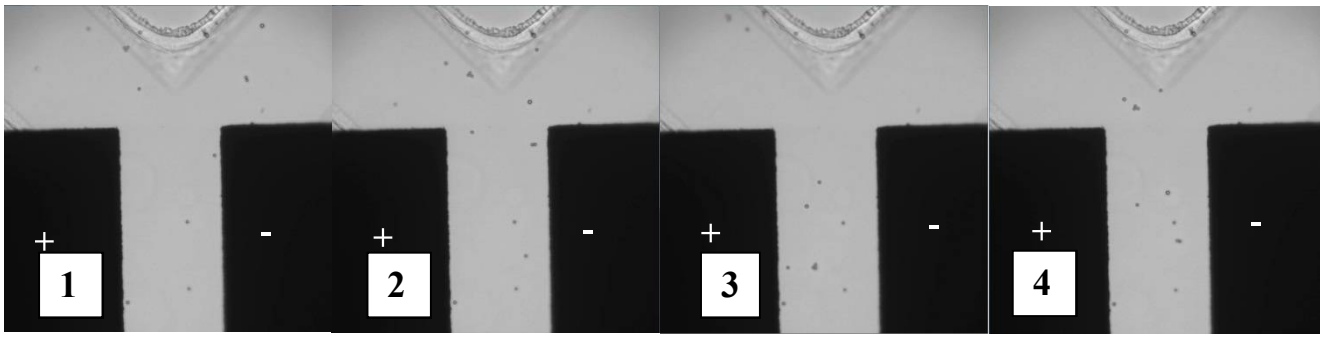

(d)

Figure 8. Examination of microfluidic devices with the negatively charged TiO_2-coated Ps beads with Ps-bead size 5.98 μm diameter. (a)-(d) represent the microfluidic devices with various distances between the microelectrodes from 30, 50, 100, 200μm, respectively. Fig. (1) at each device represents stage of devices with no electricity supplied, and Fig. (2) – (4) of each device were recorded after 1V potential is applied at the average time of 0.15, 0.40 and 0.51 sec, respectively.

Table 3. Validations of separation the negatively charged TiO_2-coated Ps-beads with various distances between the microelectrodes of microfluidic devices.

Distance of Electric fields (μm)	Electrical displacement field (c/m^2)	Moving left	Moving right	Validation
30	2.88×10^{-7}	17	3	82.35%
50	2.33×10^{-7}	20	5	75.00%
100	3.32×10^{-7}	23	3	86.96%
200	1.02×10^{-7}	19	8	57.89%

Moreover, another design of the microfluidic device has been established based on the previous designed 100 μm distance between the microelectrodes. The device is simplified to be single path. The structure is designed as shown in Figure 9. The result of examination of the single path device shows improved percentage of validation at 92.59% as shown in the table 4.

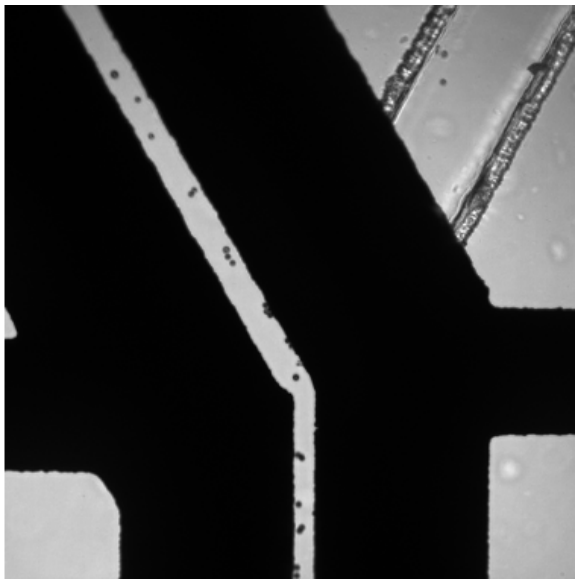

Figure 9. Examination of single path microfluidic devices with the negatively charged TiO_2-coated Ps beads with Ps-bead size 5.98 μm diameter

Table 4.. Validation of separation the negatively charged TiO_2-coated Ps-beads with the single path model of the microfluidic device.

Structure	Left	Right	Validate
Single path with 100 μm distances between the electrodes	45	2	92.59%

4. Conclusion

To avoid the ethical problems for examination the microfluidic devices with actual spermatozoa, negatively charged TiO_2-coated Ps-beads were crafted by sputtering and O_2 plasma techniques. The beads were characterized using XRD, SEM-EDS, and XAS. XRD reveals the amorphous structure on the surface of the Ps-beads. SEM images revealed that the beads were partly coated with thin shell of TiO_2 which is confermed with SEM-EDS elucidated the elemental identification of Ti and O in the coated area but cannot detect Ti anywhere else. Furthermore, structural analysis using XAS reported the TiO_2 on the Ps-beads to be likely in the amorphous form of Ti^{4+} consistence with the result of XRD. The structure of the mixed amorphous TiO_2 may be the key to maintaining the negative charge on the surface of the coated Ps-beads. Therefore, this method to fabricate the negatively charged TiO_2-coated Ps-beads can be established as the simply but efficient process to synthesize mimic charged particles on other purpose of experiment with microfluidic devices later. For the examination of the microfluidic device, the microfluidic chips were

simulated and fabricated with various distances between the electrodes at 30, 50, 100, 200 μm, respectively. After applying with 1 V electricity, the chip with 100 μm distance between the microfluidic device exhibited excellent capability to separate the negatively charged TiO_2-coated Ps-beads with 86.96% of validation and induced them into the different path of microchannel. Moreover the single path prototype of microfluidic device with 100 μm distance between the microelectrodes has been established. The percentage of validation of this device is improved to be 92.59%. Later these microfluidic devices can be tested with the actual sperm for purpose of sexual separation.

Acknowledgments

The Thailand Research Fund (TRF), through the Research and Researchers for Industries (RRI), PhD Program (PHD5710053), provided the financial support.

References

[1] Keith A, Frey MD 2010 Male reproductive health and infertility Primary Care. 37: 643.

[2] Cooper TG, Noonan E, von Eckardstein S, Auger J, Baker HW, Behre HM, Haugen TB, Kruger T, Wang C, Mbizvo MT, Vogelsong KM 2010 World Health Organization reference values for human semen characteristics Hum. Report. Update. 16: 231.

[3] Palermo G, Joris H, Devroey P, Van Steirteghem AC 1992 Pregnancies after intracytoplasmic injection of single spermatozoon into an oocyte Lancet. 340:17.

[4] O'Connell M, McClure N, Lewis S.E.M. 2002 The effects of cryopreservation on sperm morphology, motility and mitochondrial function Hum. Reprod. 17:704.

[5] Yan G, Wenjie L, Dimitri P 2013 Recent advances in microfluidic cell separations Analyst. 138:4714.

[6] Yi Z, John N, Yuan W, Yu S 2013 Recent advances in microfluidic techniques for single-cell biophysical characterization Lab Chip. **13**:2464.

[7] Niels H, Sebastian C.B, Flavio H, Andrea H 2014 Characterization of subcellular morphology of single yeast cells using high frequency microfluidic impedance cytometer Lab Chip. 14:369.

[8] Urban S, Shady G, Robert J, Arnaud B, Philippe R 2004 Cell immersion and cell dipping in microfluidic devices Lab Chip. 4:148.

[9] Ethan F, Sterling M, Jonathan Y, Saltanat N, Peter Z, Robert W 2006 Microfluidic techniques for single-cell protein expression analysis Clin. Chem. 52:1080.

[10] Ute Engelmann, Franz Krassnigg, Harald Schatz, and Wolf-Bernhard Schill, 1988 Separation of Human X and Y Spermatozoa by Free-Flow Electrophoresis, Gamete Research 19:151-159.

[11] Lang Rao, Bo Cai, Jieli Wang, QianfangMeng, Chi Ma, Zhaobo He, Junhua Xu,Qinqin Huang, Shasha Li, Yi Cen, ShishangGuo, Wei Liu, and Xing-zhong Zhao, 2015 A microfluidic electrostatic separator based on pre-charged droplets, Sensors and Actuators B 210: 328-335

[12] Farges, François, Gordon E. Brown Jr, and John J. Rehr. Coordination chemistry of Ti(IV) in silicate glasses and melts: I. XAFS study of titanium coordination in oxide model compounds. *Geochimica et Cosmochimicaacta* 60, no. 16 (1996): 3023-3038.

[13] Farges, François, Gordon E. Brown, and J. J. Rehr. Ti K-edge XANES studies of Ti coordination and disorder in oxide compounds: Comparison between theory and experiment. *Physical Review B* 56, no. 4 (1997): 1809.